Optical Properties of Circulating Human Blood

A. Roggan[1], M. Friebel[2], K. Dörschel[1], A. Hahn[3], G. Müller[1,2]

[1]Institut für Medizinische/Technische Physik und Lasermedizin, Universitätsklinikum Benjamin Franklin
Freie Universität Berlin, Krahmerstr. 6-10, D-12207 Berlin
Phone: ++49-30-8449-2327, Fax: ++49-30-8449-2399

[2]Laser- und Medizin-Technologie gGmbH, Berlin

[3]Stöckert Instrumente GmbH, München

ABSTRACT

We investigated the optical properties μ_a, μ_s, and g of human blood under flow conditions using integrating sphere measurements and inverse Monte-Carlo-simulations. The experiments were conducted at 633 nm with regard to the influence of the most important physiological and biochemical blood parameters. In addition, a spectrum of all three parameters was measured in the wavelength range 400 to 2500 nm for oxygenated and deoxygenated blood.

1. INTRODUCTION

As given by transport theory, the optical parameters are defined by the absorption coefficient μ_a [mm^{-1}], the scattering coefficient μ_s [mm^{-1}] and the anisotropy factor g in combination with a scattering phase function $p(s,s')$. Knowledge about the optical parameters of blood plays an important role for many diagnostic and therapeutic applications in laser medicine and medical routine diagnosis. For a number of optical methods the optical properties of blood are required to calculate the light distribution in blood perfused tissues, such as optical tomography, optical biopsy, diaphanoscopy, photodynamic therapy, laser induced thermotherapy, or haemangioma treatment. Human whole blood consists of 55 vol-% plasma (90 % water, 10 % proteins) and 45 vol-% cells (99 % red blood cells 'erythrocytes', 1 % leukocytes and thrombocytes). A red blood cell (RBC) has a characteristic flat biconcave form with a diameter of 7-8 µm and a thickness of 2 µm. The RBC has a mean volume of 90 μm^3 and contents 30 pg haemoglobin that allows oxygen transport. The cell concentration in blood under physiological conditions is approx. $5 \cdot 10^{12} L^{-1}$.

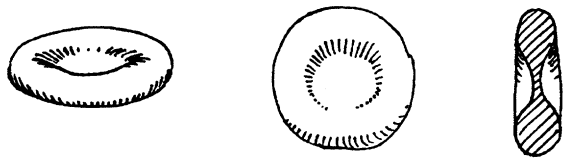

Fig. 1: Human erythrocyte

However, only few theoretical and experimental studies about the optical properties of blood have led to reasonable results because the optical properties of blood mainly depend on physiological and biochemical parameters such as haematocrit, flow, osmolarity, haemolysis and oxygen saturation. Haematocrit (hct) is the volume fraction of cells within the whole blood volume and ranges from 36.8 to 49.2 % under physiological conditions. The haemoglobin concentration ranges from 134 to 173 g/L for whole blood and from 299 to 357 g/L for RBCs. Flow induced shear stress can influence phenomena such as sedimentation, reversible agglomeration, axial migration or cell deformation and orientation. The flow parameters depend on the blood viscosity and they are influenced by the fact that blood is not a Newton fluid. A change in osmolarity induces a variation of the RBC volume due to water exchange and therefore has an impact on the haemoglobin concentration within the RBC. Haemolysis is coupled with the damage of RBC membranes by mechanical or chemical impact with consecutive release of haemoglobin into the plasma. Finally, oxygenation of haemoglobin leads to characteristic changes in its absorbing behaviour. This effect is applied in blood oxymeters.

Part of the SPIE Conference on Optical Diagnostics of Biological Fluids III • San Jose, California, USA • January 1998
SPIE Vol. 3252 • 0277-786X/98/$10.00

All mentioned parameters have to be precisely controlled during optical measurements and the blood has to be kept moving to avoid sedimentation and clustering. A physiological flow is correlated with a shear rate of approximately 500 s^{-1} in the capillary system. Therefore an experimental set-up was realised to provide measurements of the optical blood properties in the wavelength range 400 to 2500 nm under flow conditions using a specially designed flow cuvette in combination with an extracorporal circulation and oxygenation unit.

2. MATERIAL AND METHODS

2.1 Blood preparation

Fresh erythrocyte concentrates from human donors were centrifuged three times and washed in phosphate buffer solution (300 mosmol/L, pH 7.4). By doing this the blood samples contained no plasma proteins, leukocytes or thrombocytes. Light microscopy control of the samples ensured that they were neither haemolysed nor were the cells deformed. The haematocrit (hct) was used as a measure for the concentration of red blood cells and was adjusted by diluting with phosphate buffer. In the present experiments blood samples were investigated with a haematocrit value of 2.5 to 70 %. Dilution with buffer of different osmolarities allowed the adjustment of various blood osmolarities from 225 to 450 mosmol/L. In addition, a quantitative haemolysis was induced by diluting with distilled water.
Blood circulation and predetermined oxygen states were adjusted with an extracorporal circulation unit (Fa. Stöckert Instrument GmbH). The blood was gently stirred and kept flowing through a specially designed turbulence free cuvette with an laminar flow and an optical path of 97 µm (Fig. 2). Oxygen saturation was adjusted by continuous flow of a mixture of O_2, N_2 and CO_2 through a modified membrane oxygenator. The oxygen saturation was continuously controlled by a blood oxymeter (OxySAT-Meter SM 0200; Baxter). For complete deoxygenation the erythrocyte concentrates were diluted with phosphate buffer containing 0.3 % sodium dithionite ($Na_2S_2O_4$). With the exception of experiments based on changing oxygen states all investigations were derived with an oxygen saturation over 98 %. The blood temperature was kept constant at 20°C.

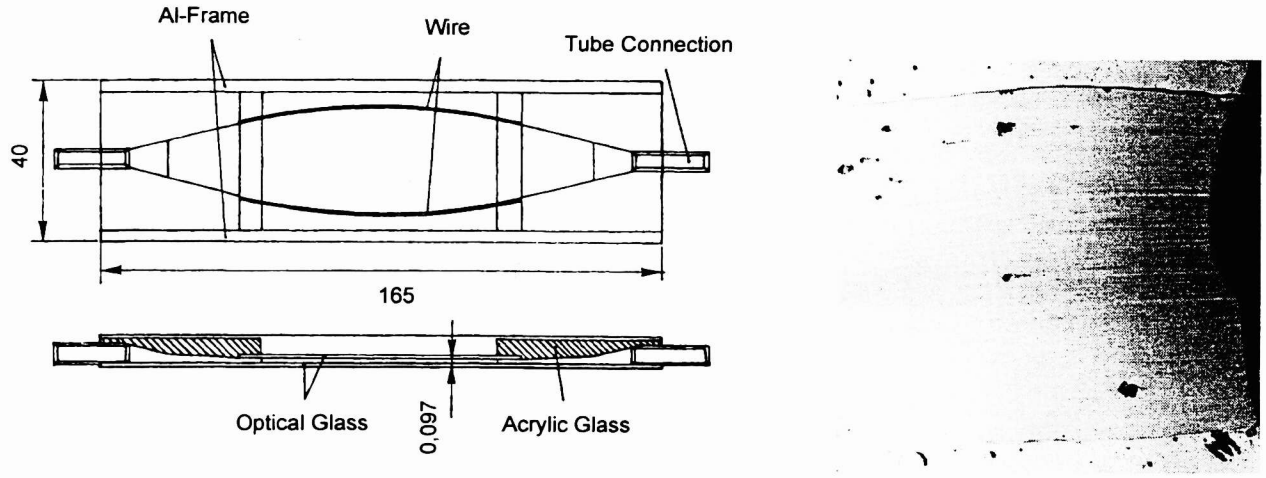

Fig. 2: Turbulence free flow cuvette with a thickness of 97 µm

2.2 Experimental set-up

The optical properties of scattering and absorbing media cannot be measured directly. As a result, the blood properties were determined by double integrating sphere technique, evaluating the diffuse backscattering R_d, the total transmission T_t, and the collimated, i.e. non-scattered transmission T_c of thin samples[1,2,3] (Fig. 3 left). The inner surfaces of the integrating spheres (∅152 mm) were coated with a highly reflecting layer of Spectralon®, allowing the total radiation in the hemispheres in front and behind the sample to be collected. Reflection standards were used to calibrate the system (Labsphere).

All measurements with respect to varying physiological blood parameters were carried out at a fixed wavelength of 632.8 nm, using a Helium-Neon Laser with 1.2 mW output power (Spindler & Hoyer). The spot size on the sample was Ø7 mm, the distance between sample and T_c-detector was 1330 mm. The aperture in front of the T_c-detector was Ø5 mm, the beam diameter in the aperture plane was Ø1.2 mm. A mercury high pressure short arc lamp served as light source for the spectral overview of optical properties (Osram, 100 watts, $2 \cdot 10^6$ cd/cm^2). The lamp was connected to a monochromator (AMKO, f=200 mm) with a resolution of 8 nm (FWHM) in the range 400-1140 nm and 16 nm (FWHM) in the range 1140-2500 nm. The circular monochromator exit slit (Ø1 mm) was focused on the flow cuvette, providing a spot size of Ø4 mm. The distance between sample and T_c-detector was 430 mm, the aperture in front of the T_c-detector was Ø30 mm, the beam diameter in the aperture plane was Ø25 mm. The beam was mechanically chopped at 220 s^{-1} and part of the beam was used for the reference intensity compensation. Silicon photodiodes (AMKO, 09-SiU04-C, 400-1140 nm) and lead sulphide photodiodes (AMKO, 09-Pb01-C, 1140-2500 nm) were used as detectors. The signals were finally recorded with lock-in technique (ITHACO 3981).

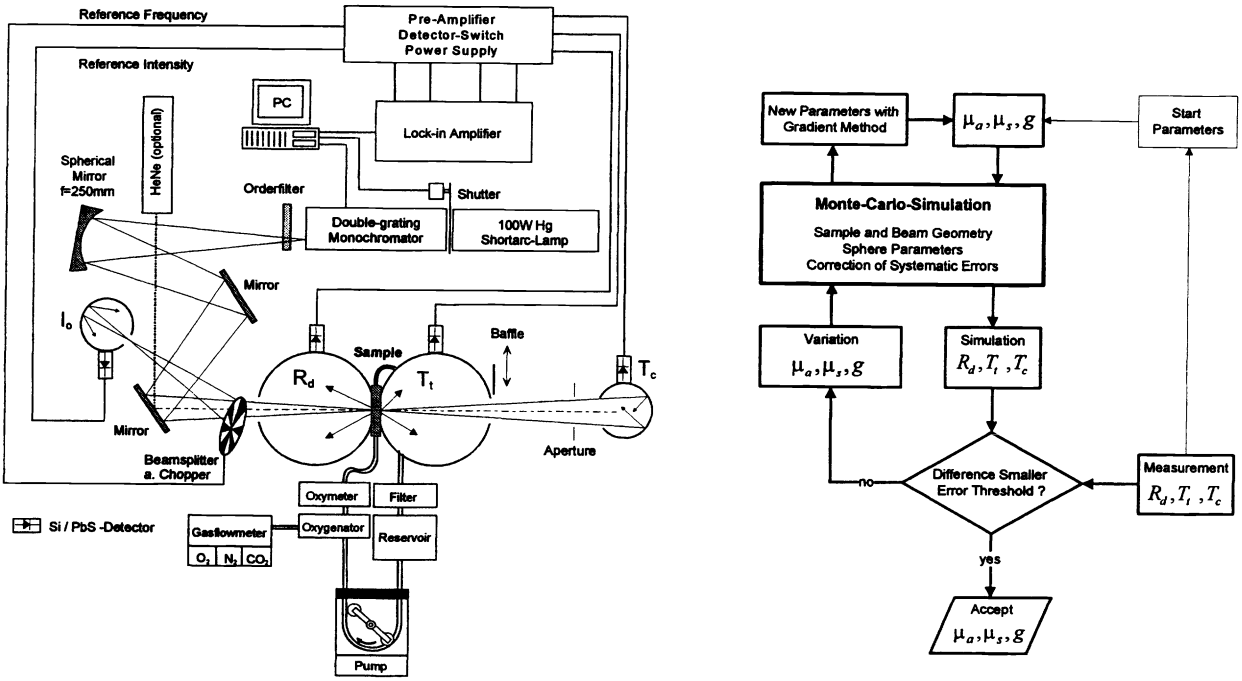

Fig. 3: Experimental set-up for the determination of optical properties of human blood (left), scheme of the inverse Monte-Carlo simulation for the calculation of optical properties from measured data (right)[1,2,3]

2.3 Evaluation of optical properties

The extraction of the optical parameters μ_a, μ_s, g from the measurements is a complex task as there are no analytical models available with sufficient precision. The method of choice was therefore the Monte Carlo Simulation, which as a statistical method calculates the trajectories of a great number of photons ($3 \cdot 10^5$ in our experiments) and as a result presents the remission and transmission characteristics of a sample for a given set of optical parameters. In order to solve the opposite situation, i.e. to determine the unknown optical parameters from the measured macroscopic values, the Monte Carlo simulation must be inverted[1,2,3] (Fig. 3, right). For this the measured data were simulated taking an estimated set of start parameters μ_a, μ_s, g from Kubelka-Munk theory[4]. Then the measured quantities were calculated and compared with the real measurement. In case of a significant deviation all three parameters were varied slightly and three new forward simulations were performed. After this procedure a gradient matrix was built up, allowing the calculation of new optical parameters which fit better to the measured quantities. This procedure was repeated until the deviation between measured and calculated values was within the error threshold (0.1 %). Thus the associated set of optical parameters could be accepted. As well as a high degree of accuracy the method offers a simple means of compensating systematic errors such as

radiation losses, scattered photons detected at the T_c-detector, deviations from a Lambertian distribution of the diffuse reflectance, and an incomplete separation of the radiation fields in the integrating spheres. The potential disadvantage of long calculation times could be compensated for by the use of currently available fast computer systems (Pentium 200 MHz).

One of the most important points when dealing with Monte-Carlo-simulations of photon transport in turbid media is the choice of a scattering phase function that fits best to the investigated medium. Therefore the Henyey-Greenstein phase function is most often used in biomedical optics because of its good correspondence to goniophotometric measurements of tissues like skin or parenchymatous organs[5-14]:

$$p_{HG}(\mathbf{s},\mathbf{s}') = \frac{1-g_{HG}^2}{4\pi\left(1+g_{HG}^2-2g_{HG}\cos\Theta\right)^{3/2}}$$

Here $p_{HG}(\mathbf{s},\mathbf{s}')$ is the normalised probability for a photon to be scattered from a direction **s** into a direction **s'**, g_{HG} is the free parameter which equals the mean cosine of the scattering angle, known as the anisotropy factor g. On the other hand it is known that the Henyey-Greenstein phase function does not fit to the scattering of RBCs because of their large diameter. Therefore Yaroslavsky proposed the Gegenbauer-Kernel phase function for blood samples[15]. This is a two parameter function with $\alpha_{GK}>0$ and $-1 \le g_{GK} \le 1$. The Gegenbauer-Kernel phase function equals the Henyey-Greenstein phase function for $\alpha_{GK}=0.5$, the anisotropy factor g has to be calculated numerically:

$$p_{GK}(\mathbf{s},\mathbf{s}') = \frac{\alpha_{GK} g_{GK}}{\pi\left(\left(1+g_{GK}\right)^{2\alpha_{GK}}-\left(1-g_{GK}\right)^{2\alpha_{GK}}\right)} \cdot \frac{\left(1-g_{GK}^2\right)^{2\alpha_{GK}}}{\left(1+g_{GK}^2-2g_{GK}\cos\Theta\right)^{\alpha_{GK}+1}}$$

The importance of a correct phase function becomes evident with regard to photons which travel trough the measuring cuvette and which are scattered only once or twice. These photons have a high probability to be collected in the T_c-detector because of the extreme forward scattering of RBCs. Thus these photons had to be considered as a T_c-offset in the Monte-Carlo routine, but the amount of this offset strongly depended on the selected phase function. This is shown in figure 4 where three phase functions with the same anisotropy factor of g=0.9924 are compared. Mie calculations of the RBC phase function at 633 nm served as a reference where a mean diameter of 5.56 µm was selected as a spherical RBC equivalent with a volume of 90 μm^3. The refractive index was set to n=1.333 for the surrounding medium and to n=1.402 for the RBC. That the Mie calculation for a spherical equivalent is a valid assumption for RBCs could be shown in the subsequent measurements at various plasma osmolarities (see 3.3 and 3.4 for detailed information).

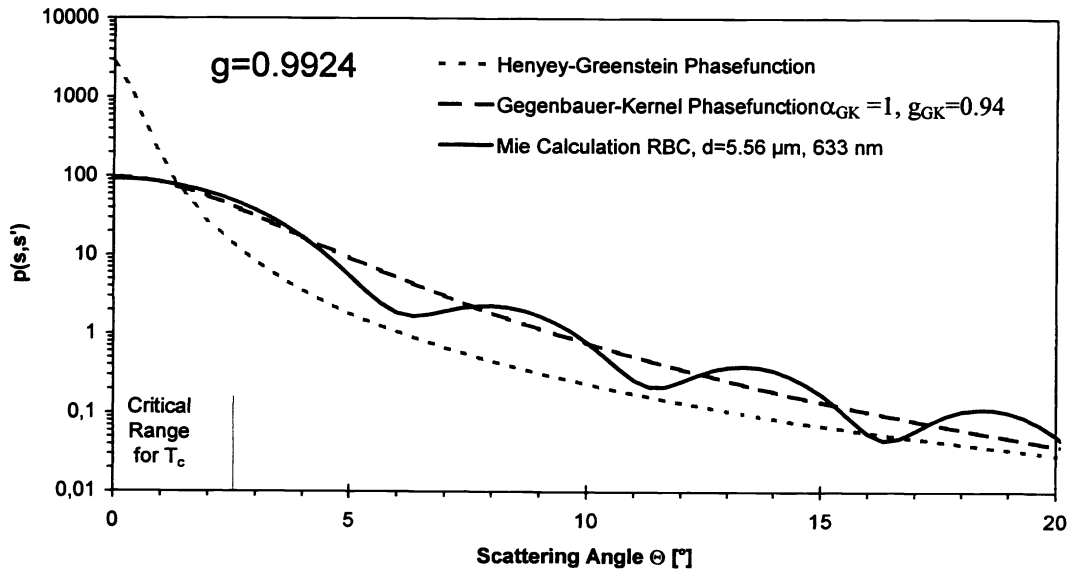

Fig. 4: Comparison of various phase functions for red blood cells

Evidently the Henyey-Greenstein phase function overestimates the RBC phase function by a factor of over 10 within the first degrees of the scattering angle that are critical for the T_c-detection. On the other hand, the Gegenbauer-Kernel phase function with α_{GK} =1.0 mimics the Mie function without significant deviations in the critical range. Therefore the Gegenbauer-Kernel phase function was implemented in the Monte-Carlo model and a fixed factor of α_{GK} =1 was applied for all subsequent evaluations while the factor g_{GK} was the free fit parameter. The anisotropy factor g was finally calculated numerically.

2.4 Execution of measurements

For each experimental question a total of three independent measurement series were carried out using erythrocyte concentrates from different human donors. One measurement series at a fixed wavelength of 633 nm with varying haematocrit, shear rate, osmolarity, haemolysis or oxygenation required approximately 60 minutes. The evaluation of the optical properties applying inverse Monte-Carlo simulations required a total time of 10-20 hours for all three series of one experiment. Mean values and standard deviations were calculated as shown in the subsequent graphs. The spectral overview required approximately 5 hours for each spectrum that was also measured three times in order to calculate mean values of optical properties. Before and after each measurement the blood samples were checked for their haematocrit as well as for possible haemolysis and cell deformation.

3. RESULTS AND DISCUSSION

3.1 Haematocrit

Isotonic blood samples (300 mosmol/L) of various haematocrits were measured at a wavelength of 633 nm. Fig. 5 shows the mean values (n=3) of μ_a, μ_s, g and μ_s' depending on the haematocrit ranging from 0 to 70 % at a constant shear rate of 500 s^{-1}. The absorption coefficient μ_a increased linearly with the haematocrit over the whole measured haematocrit range. The scattering coefficient μ_s also increased proportionally to the haematocrit but only for values of hct $\leq$ 10 %. The anisotropy factor g was almost constant in that haematocrit range (0.994>g>0.992). On the other hand, μ_s appeared to be independent of blood concentration at values hct>10 % and the g factor decreased continuously down to 0.975 at hct 70 %. Investigating the measured quantities (Fig. 5), one could conclude that the collimated transmission dropped below the detection threshold for hct>10 %. Therefore the calculation of three independent optical properties was not possible and consequently the reduced scattering coefficient $\mu_s'=\mu_s(1-g)$ was evaluated. In contrast to μ_s a linear increase was found for μ_s' up to hct 45 %. Above 45 % a slight saturation effect was found which might be the result of either interfering scattering events or the formation of two or more RBCs to a clusters. This non-linear scattering dependence on haematocrit was already predicted by Reynolds from theoretical investigations[16]. Due to the incomplete separation of μ_s and g only μ_s' was calculated for blood samples at haematocrits above 10 %.

3.2 Flow velocity

The optical properties were measured under various flow conditions to derive the effects of blood flow on μ_a and μ_s' (Fig. 6). The underlying mechanism of cell deformation and axial migration is the predominating shear force within the flow cuvette. Therefore the shear rate was calculated from the ratio of flow velocity and cuvette cross section. The range of the adjusted shear rate corresponded to the physiological range in the human vascular system. A low shear rate of 50 s^{-1} led to a decrease of μ_a to 95 % compared to a short flow stop. Additional increase of the shear rate resulted in a continuous but smaller decrease of μ_a down to 88 % at γ=3000 s^{-1}. The reduced scattering coefficient μ_s' showed a similar behaviour with increasing shear rates. μ_s' decreased to 93 % at γ=50 s^{-1} and to 80 % at γ=3000 s^{-1}. It could be clearly shown that the flow velocity and the related shear rates had a significant impact on the optical properties of blood. However, from the measured data it was not possible to differentiate if the shear rate dependence was a result of cell deformation or axial migration. Thus, further measurements with different geometrical shapes of RBC were carried out by varying the osmolarity of the buffer.

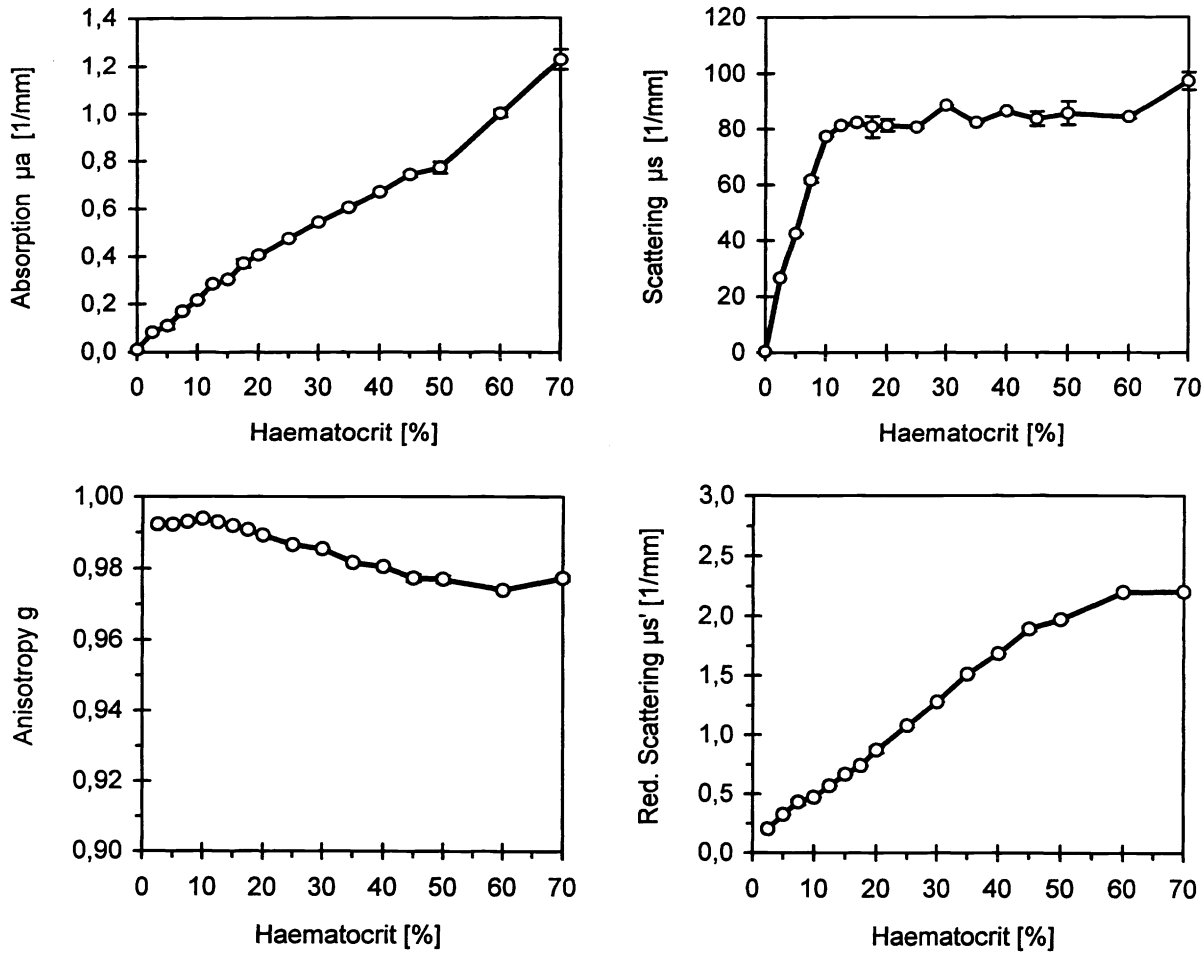

Fig. 5: Mean values ± SD (n=3) of μ_a, μ_s, g and μ_s' versus haematocrit (π=300 mosmol/L, γ=500 s^{-1}, $SatO_2$>98 %, λ=633 nm)

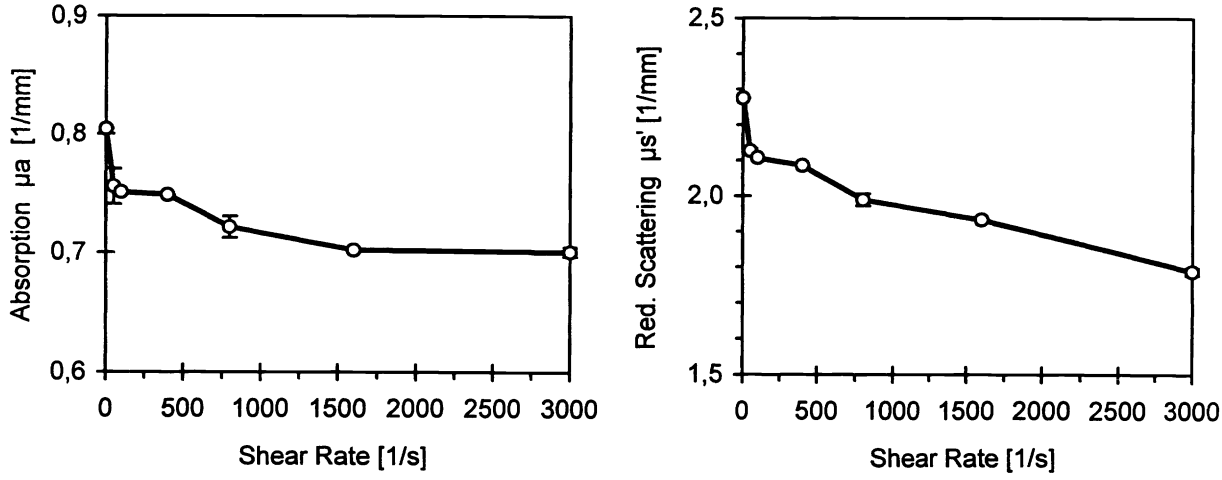

Fig. 6: Mean values ± SD (n=3) of μ_a and μ_s' versus shear rate (hct=41 %, π=300 mosmol/L, γ=500 s^{-1}, $SatO_2$>98 %, λ=633 nm)

3.3 Osmolarity

Variation in the plasma osmolarity lead to considerable changes in the shape of the erythrocytes. Hyper-osmotic plasma induces cell shrinking (acanthocytes), in hypo-osmotic plasma the cells swell (spherocytes). In both cases deformability of the erythrocyte is distinctly diminished. Diluted blood samples (hct=7.5 % at 300 mosmol/L) were adjusted to osmolarity values ranging from 225 to 450 mosmol/L using phosphate buffer solutions of various osmolarity. Because the number of cells per volume was kept constant for these experiments the haematocrit varied slightly with osmolarity due to the different cell volumes. Fig. 7 shows the measured optical properties at a wavelength of 633 nm.

The absorption coefficient μ_a increased continuously with osmolarity, i.e. cell shrinking led to an increase of μ_a. At 225 mosmol/L μ_a amounted to 60 % of the value measured under isotonic conditions while μ_a was 50 % above the isotonic value at 450 mosmol/L. This effect was unexpected because the number of cells, and therefore the overall concentration of absorbing haemoglobin, was kept constant during all measurements with different osmolarities. An explanation will be given in the discussion of the measurements on haemolysed blood samples.

The scattering coefficient μ_s showed a slight decrease with increasing osmolarity of about 10 %. Also the anisotropy factor g decreased from 0.995 at 225 mosmol/L down to 0.991 at 450 mosmol/L. The reduced scattering coefficient μ_s' increased linearly with osmolarity. In contrast to the absorption properties, the scattering behaviour appeared to be reasonable because the cell shape and the refractive index of the cell bounded haemoglobin solution varied with osmolarity, both strongly affecting the scattering performance.

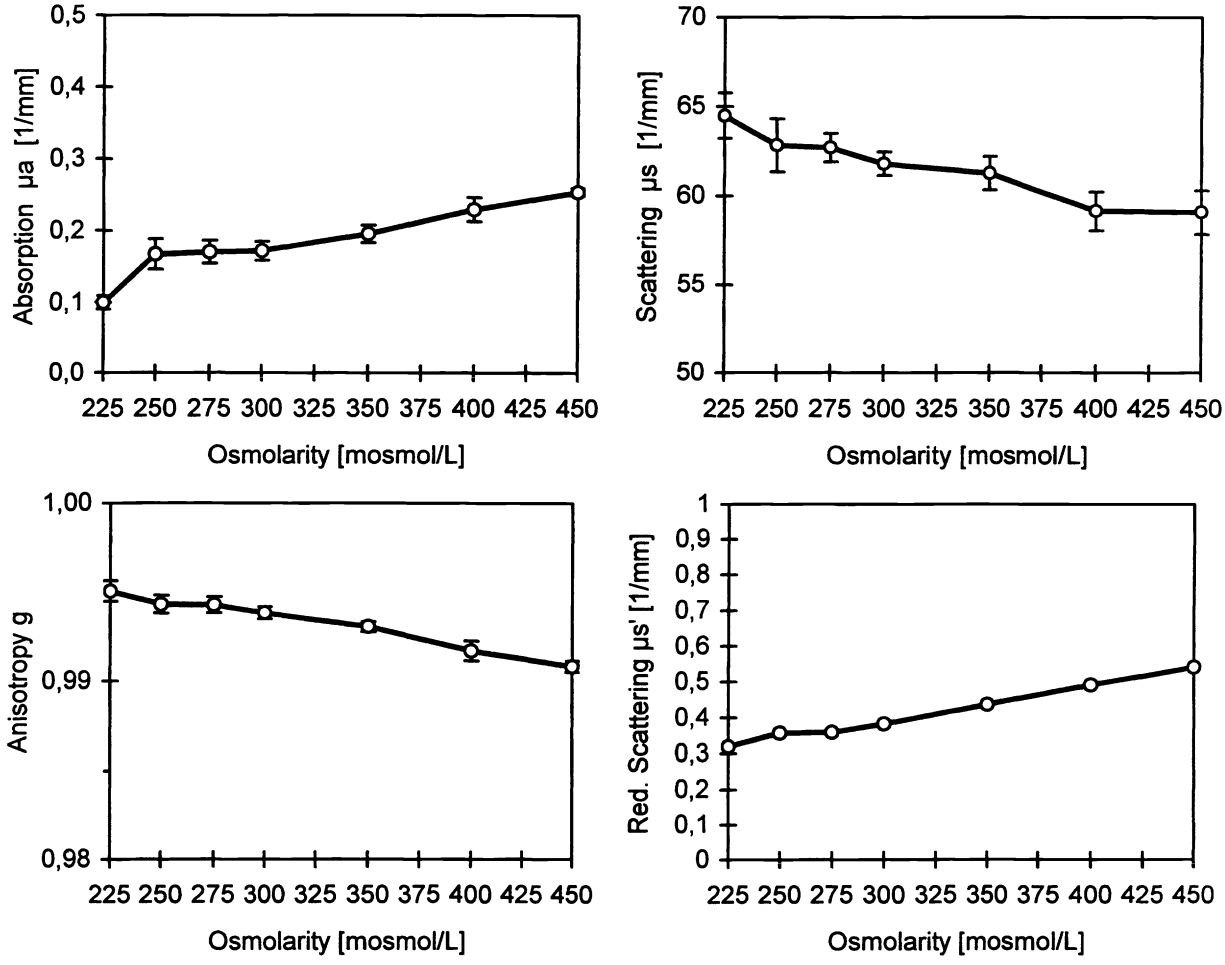

Fig. 7: Mean values±SD (n=3) of μ_a, μ_s, μ_s' and g at short flow stop versus plasma osmolarity (hct=7.5 % at 300 mosmol/L, γ=0 s^{-1}, $SatO_2$>98 %, λ=633 nm)

Mie calculations on red blood cells were carried out applying the algorithms of Zijp and ten Bosch[17,18] to differentiate between the impact of cell shape and refractive index. Therefore the cell shape was assumed to be spherical when applying Mie theory and the sphere diameter was adjusted to mimic the RBC volume coupled to a certain osmolarity. The refractice index of the surrounding buffer was set to n_{water}=1.333, the refractive index of the cell bounded haemoglobin solution was derived by the equation $n_{solution} = n_{water} + \beta \cdot c$, where c is the haemoglobin concentration in g/100 ml and β=0.001942 at a wavelength of 589 nm[19]. Assuming a mean erythrocyte volume of 90 μm^3 and an inner cell haemoglobin concentration of 350 g/L (35 g/100 ml) for isotonic conditions, a refractive index of n_{300}=1.402 and a sphere equivalent diameter of d_{300}=5.56 µm can be calculated. Considering slight variations of the haematocrit at 250 mosmol/L (hct 8.1 %, RBC volume 96,7 μm^3, RBC haemoglobin concentration 325 g/L) and 400 mosmol/L (hct 6.6 %, RBC volume 78,6 μm^3, RBC haemoglobin concentration 400 g/L) the corresponding refractive indices are n_{250}=1.397 and n_{400}=1.412 and the sphere equivalent diameters are d_{250}=5.70 µm and d_{400}=5.32 µm. The scattering coefficients were calculated by multiplying the Mie scattering cross section with the number density of $8.33 \cdot 10^{11}$ L^{-1} which is related to hct=7.5 % at 300 mosmol/L and which was kept constant at all osmolarities.

Fig. 8 shows the results of the Mie calculations for μ_s and g compared with the measured data. At 250 mosmol/L μ_s is calculated to be 63.8 mm^{-1} versus 62.8±1.5 mm^{-1} for the measured value, at 300 mosmol/L 62.2 mm^{-1} versus 61.8±0.7 mm^{-1} and 57.7 mm^{-1} versus 59.1±1.1 mm^{-1} at 400mosmol/L. The calculated values of g are 0.994 versus 0.9943±0.0005 at 250 mosmol/l, 0.9924 versus 0.9938±0.0004 under isotonic conditions and 0.990 versus 0.9917±0.0006 at 400 mosmol/L. The agreement of measurements and calculations indicate that the form of the erythrocytes is of minor importance for the scattering properties of blood. Variations in the scattering behaviour are due to changes in cell volume and refractive index. In addition, these results indicate that the dependence of the absorption and scattering behaviour on shear rate was mainly caused by a dynamic decrease of haematocrit as a result of axial migration (Fahraeus effect), while shear stress induced cell deformation can be neglected with respect to the optical properties.

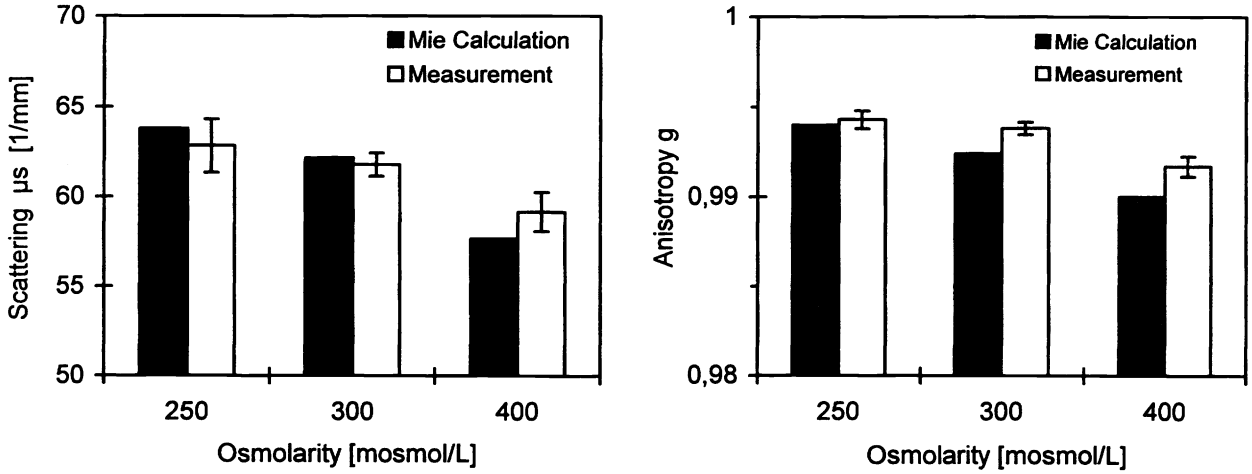

Fig. 8: Measured mean values ± SD (n=3) of μ_s and g compared with Mie calculations for spherical equivalents (hct=7.5 % at 300 mosmol/L, γ=0 s^{-1}, $SatO_2$>98 %, λ=633 nm)

3.4 Haemolysis

Blood samples of different haemolytic states were prepared by mixing intact and completely haemolysed blood without removing the membrane residuals. Fig. 9 shows the measured optical properties at five different degrees of haemolysis between 0 and 100 %.

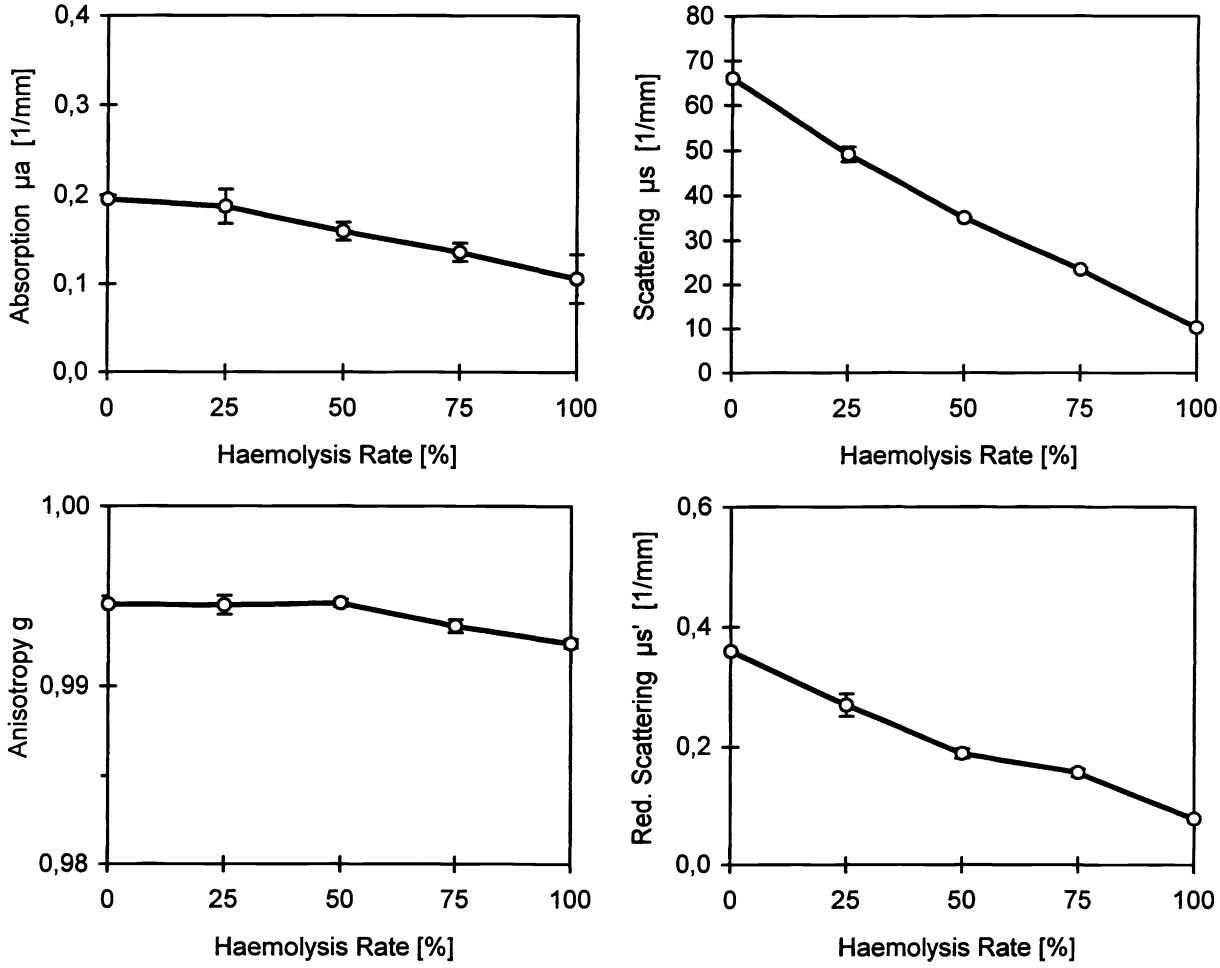

Fig. 9: Mean values ± SD (n=3) of μ_a, μ_s, g and μ_s' versus extent of haemolysis (hct=7.5 %, π=300 mosmol/L, γ=500 s^{-1}, $SatO_2$>98 %, λ=633 nm)

The absorption coefficient μ_a significantly decreased with increasing haemolysis. When blood was completely haemolysed, μ_a amounted 0.11±0.03 mm^{-1} which was only 46 % of the value for intact blood (0.20±0.05 mm^{-1}). Nevertheless, the dependence of haemoglobin absorption on haemolysis rate was as unexpected as the increase of absorption with increasing osmolarity because the overall haemoglobin concentration was kept constant. The fact that absorption is higher in blood than in a haemoglobin solution with the same concentration can also be found by comparing literature data and scaling the reported absorption coefficients to our concentration of 27 g/L (Hct=7.5 %). For an oxygenated haemoglobin solution Gordy[20], Steinke[21] and Kuenstner[22] reported a mean μ_a of 0.064±0.013 mm^{-1} at 633 nm. On the other hand, Reynolds[16] and Steinke[24] reported a mean μ_a of 0.12±0.04 mm^{-1} for whole human blood. The values are slightly smaller than our data but the same factor of approximately two can be deduced.

The scattering coefficient μ_s showed a distinct decrease with increasing haemolysis. At complete haemolysis μ_s amounted to 18 % of the value measured for intact blood. The anisotropy factor g was constant up to 50 % haemolysis and slightly decreased at higher haemolysis rates. μ_s' decreased continuously reaching values of about 16 % compared to intact blood. The decrease of scattering with increasing haemolysis rate followed from the fact that destroyed erythrocytes distributed their haemoglobin into the whole solution, resulting in a refractive index match. Thus the RBCs loose their scattering properties. Consequently the measurements showed that the residual erythrocyte membranes have only a minor impact on the scattering properties what might be understood from their very small wall thickness of about 4 nm.

Even more remarkable was the significant decrease in absorption when blood was haemolysed or osmolarity was decreased. This phenomenon found an explanation in the special scattering and absorbing structure of blood. Here scattering cannot be assumed to occur at point scatterers with absorption taking place in the surrounding (non scattering) medium. In blood the scatterers themselves have a significant dimension compared to the whole volume and they contain all or at least part of the absorbers. Hence it has to be taken into consideration that the optical path of a photon within a scatterer might be increased due to multiple reflections at its internal boundary ('caught' photon, fig. 10). This effect of internal reflections is well known from atmospherical scattering in water drops and is responsible for the occurrence of rainbows. The increased pathlength on its part leads to a higher absorption probability of the whole solution if absorbers are contained within the scatterers. Consequently, this results in a decrease of the overall absorption coefficient if more and more erythrocytes loose their scattering properties due to haemolysis. The phenomenon of the 'caught' photon also explains the increase of μ_a when osmolarity increases (see fig. 7). Here the RBC refractive index increased due to the higher RBC haemoglobin concentration in the hyper-osmolar state. Hence the number of internal reflections also increased, resulting in a higher total absorption coefficient. Non-linear absorption aspects as a concentration dependent extinction coefficient and the shielding effect can be excluded to describe the results because they would reduce μ_a with increasing inner cell haemoglobin concentration and not vice versa.

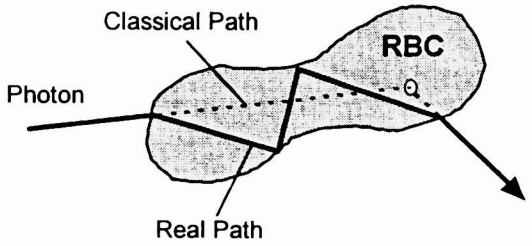

Fig. 10: Path of a photon within an erythrocyte

3.5 Oxygen Saturation

To elucidate the influence of oxygen saturation on the optical properties of blood a sample (hct 41 %) was investigated at different oxygen saturation between 100 and 30 %, adjusted by insufflation of N_2 and CO_2. Fig. 11 shows the measured values of μ_a and μ_s' versus O_2 saturation. At a wavelength of 633 nm μ_a shows a linear decrease with increasing O_2 saturation. Completely oxygenated blood shows approximately half the absorption of blood with an oxygen saturation of 30 %. The reduced scattering coefficient μs' remains constant over the measured range of oxygen saturation. As was expected, oxygenation only changed the absorption properties of blood. Scattering remained unaffected by changes in oxygen saturation.

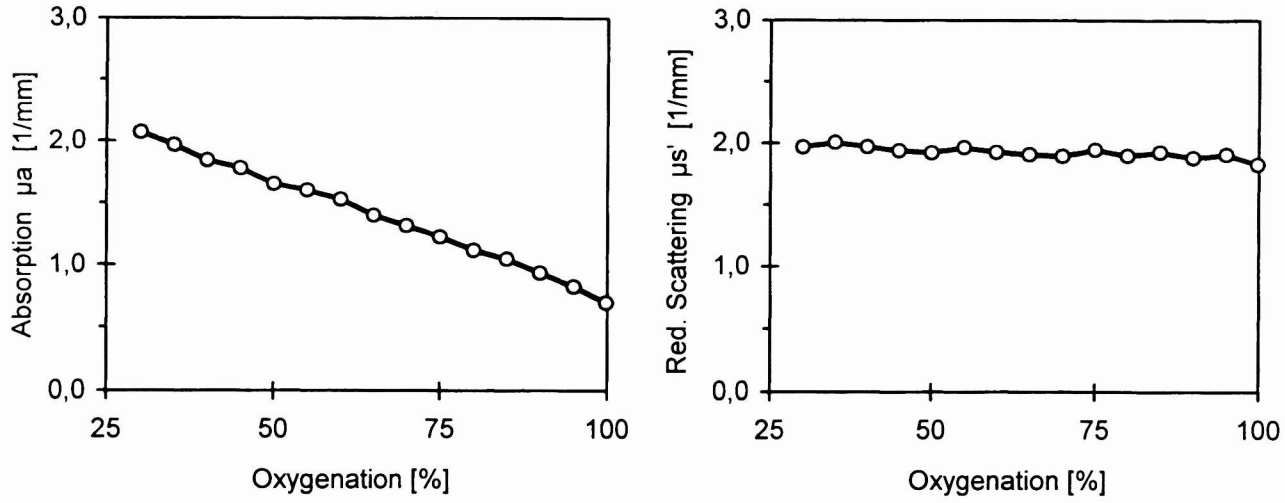

Fig. 11: Absorption coefficient μ_a and reduced scattering coefficient μ_s' versus O_2 saturation (hct=41 %, π=300 mosmol/L, γ=500 s^{-1}, λ=633 nm)

3.6 Optical properties of diluted blood in the wavelength range 400 to 2500 nm

To obtain a complete optical spectrum of blood, measurements in the wavelengths range 400 to 2500 nm were conducted in increments of $\Delta\lambda$=10 nm. Fig. 12 shows the mean values (n=3) of μ_a, μ_s and g for oxygenated isotonic blood at hct=5 % and a shear rate of 500 s^{-1}. In addition, the measurements were repeated for completely deoxygenated blood samples. Significant differences were only found for the absorption coefficient in the wavelength range of 400 to 1200 nm. Here the spectra correlated qualitatively with literature data on haemoglobin solutions[20-22]. The absorption spectra showed the well-known characteristic maximums around 420 nm and 540 nm and the isosbestic point at 805 nm. However, μ_a was approximately twice compared to the reported haemoglobin solutions if they were scaled to our measured concentration of 18 g/L (Hct=5 %). Above 1200 nm the absorption spectra of oxygenated and deoxygenated blood were not significantly different and followed the water absorption. In the range of 1170 to 1350 nm blood absorption was approximately twice that of water, above 1350 nm μ_a followed the water absorption on a level of approximately 120-130 %. Thus the same effect of increased absorption that was found in the visible region also appeared for the water absorption in the mid infrared where other absorbers are negligible. This can also be explained by the 'caught' photon phenomenon, because it does not matter whether inner cell absorption is caused by water or haemoglobin. Nevertheless the increased water absorption can only be seen if haemoglobin is present in the RBC because it is needed to increase the refractive index in comparison to the surrounding medium.

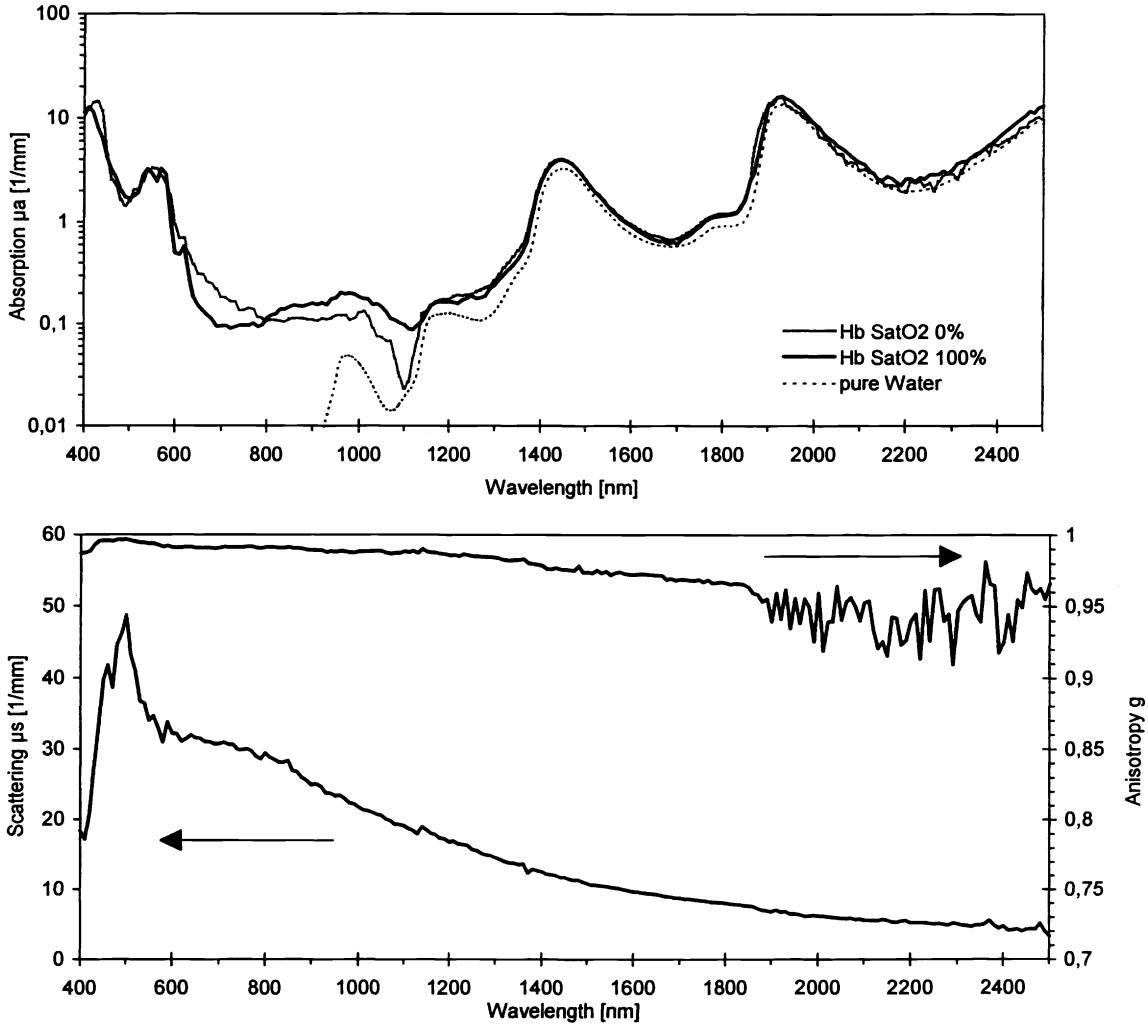

Fig. 12: The absorption spectrum of oxygenated and deoxygenated diluted blood and the values of μ_s and g which did not vary with oxygenation (hct=5 %, π=300 mosmol/L, γ=500 s^{-1})

In contrast to the absorption coefficient no differences between scattering coefficients or anisotropy factors were found for both oxygen saturations over the whole measured wavelength range. The scattering coefficient μ_s showed a distinct maximum at 500 nm with values over 40 mm^{-1} which was consistent with theoretical investigation of Pittman[23]. In the wavelength range 550 to 800 nm μ_s slightly decreased to values of 30 mm^{-1}. Above 800 nm μ_s decreased proportionally with wavelength to $\lambda^{-1.7}$. At 2500 nm μ_s amounted to 10 % of the value found at 500 nm. The decrease of μ_s with wavelength is due to a reduction of the scattering cross section and is consistent with Mie calculations. Considering the measured dilution of the investigated blood sample (hct=5 %) very high scattering coefficients above 350 mm^{-1} at 500 nm can be expected for blood with physiological concentrations (hct≈41 %).
The anisotropy factor g was larger than 0.98 in a wavelength range from 400 to 1400 nm with maximum values over 0.99 in the range 400 to 600 nm. Above 1400 nm *g* decreased slightly to values about 0.95 in the near infrared. The increasing oscillation of g above 1800 nm was caused by the small values of the measured quantities. Especially R_d was found to be far below 0.1 % in this range. These results confirm the forward scattering characteristic of blood over a wide range of wavelength.

4. SUMMARY AND CONCLUSION

Fundamental knowledge about the optical behaviour of human blood could be derived in the present study. We found that measurements under flow conditions were a necessary prerequisite to get exact and reproducible results on blood samples. The double integrating sphere technique proved to be a reliable method to determine macroscopic optical properties. It was necessary to apply inverse Monte-Carlo simulations that took into consideration all kinds of systematic errors to calculate precise intrinsic optical properties from the measured quantities. One of the most important details was the application of an optimised scattering phase function for red blood cells. We found that the Gegenbauer-Kernel phase function with $\alpha_{GK}=1$ fit best to the scattering behaviour of blood samples.
The impact of variations of the most important physiological blood parameters on the optical properties was measured at 632.8 nm using a HeNe-laser. We found that

- scattering and absorption increased linearly with haematocrit if hct<50 %
- absorption and scattering decreased slightly with increasing shear rate
- axial migration was the predominant factor on the optical properties with respect to the flow parameters
- the deformation of erythrocytes had no impact on the optical properties if volume and haemoglobin content was kept constant
- increasing osmolarity lead to an increase of absorption while scattering and anisotropy decreased
- Mie calculations on spherical equivalents provided a precise estimation of the RBC scattering behaviour
- increasing haemolysis led to a reduction in absorption and scattering
- haemoglobin solutions had a smaller absorption coefficient than whole blood at the same concentration
- the membranes of red blood cells had only a minor impact on the scattering behaviour
- oxygenation only changed the absorption properties

The spectral overview in the wavelength range 400 to 2500 nm at hct=5 % lead to the following conclusions:

- blood absorption followed haemoglobin absorption in the range 400-1200 nm on a level of approx. 200 %
- blood absorption followed water absorption at wavelength above 1200 nm on a level of 120 to 200 %
- a distinct difference between oxygenated and deoxygenated blood was only found for the absorption coefficient in the range 400-1200 nm
- scattering showed a maximum around 500 nm and decreased with wavelength at a rate of approx. $\lambda^{-1.7}$
- Anisotropy was larger than 0.99 in the range 400-800 nm, larger than 0.98 in the range 800-1400 nm and larger than 0.9 between 1400 and 2500 nm

One can conclude that scattering of blood is mainly caused by a high refractive index of the haemoglobin solution within the RBCs. Internal reflections of photons lead to an increase of the overall absorption coefficient by increasing the optical pathlength within the cells. This effect explains the difference between normal and haemolysed blood as well as the increase of absorption with increasing osmolarity and the increased water absorption in the near infrared.
From our data it is possible to calculate the optical properties of blood for any given haematocrit up to 50 % because scattering increases linearly with haematocrit and anisotropy remains unchanged. For the adaptation of the absorption coefficient it is necessary to separate between haemoglobin and water absorption.

REFERENCES

1. Roggan A., Minet O., Schroeder C., Mueller G.: Measurements of optical properties of tissue using integrating sphere technique. SPIE Institute for Advanced Optical Technologies, in: Müller G. et. Al (Eds.): Medical Optical Tomography: Functional Imaging and Monitoring. Vol. IS11:149-165 (1993)
2. Roggan A., Dörschel K., Minet O., Wolff D, Müller G.:The optical properties of biological tissue in the near infrared wavelength range - review and measurements. In: Müller G, Roggan A (Eds.). Laser-induced Interstitial Thermotherapy. SPIE Press, Bellingham, 10-44 (1995)
3. Roggan A.: Dosimetrie thermischer Laseranwendungen in der Medizin - Untersuchung der optischen Gewebeeigenschaften und mathematisch-physikalische Modellbildung. Dissertation, Technische Universität Berlin. In: Müller G., Berlien H.-P (Eds.): Fortschritte in der Lasermedizin, Bd. 16, Ecomed, Landsberg (1997)
4. Kubelka P., Munk F.: Ein Beitrag zur Optik der Farbanstriche. Z. Tech. Phys. 12: 593-601 (1931)
5. Henyey LG., Greenstein JL.: Diffuse radiation in the galaxy. Astrophysical J. 93:70-83 (1941)
6. van de Hulst HC.: Multiple light scattering. Vol. 1, Academic Press, New York (1980)
7. van de Hulst HC.: Multiple light scattering. Vol. 2, Academic Press, New York (1980)
8. Flock ST., Wilson BC., Patterson MS.: Total attenuation coefficients and scattering phase functions of tissue and phantom materials at 633 nm. Med. Phys. 14 (4): 835-841 (1987)
9. Jacques SL., Alter CA., Prahl SA.: Angular dependance of HeNe laser light scattering by human dermis. Lasers in Life Science 1(4): 309-333 (1987B)
10. Arnfield M., Tulip J., McPhee M.: Optical propagation in tissue with anisotropic scattering. IEEE Trans. Biomed. Eng. 35: 372-381 (1988)
11. Prahl S.: Light transport in tissue.Ph.D Dissertation, University of Texas at Austin (1988)
12. Marchesini R., Bertoni A., Andreola S., Melloni E., Sichirollo AE.: Extinction and absorption coefficients and scattering phase functions of human tissues in vitro. Appl. Opt. 28(12): 2318-2324 (1989)
13. van Gemert MJC., Jacques SL., Sterenborg HJCM., Star WM.: Skin optics. IEEE Trans. Biomed. Eng. 36: 1146-1154 (1989)
14. Essenpreis M., van der Zee P., Jones PS., Gewehr P., Mills TN.: Changes in scattering phase function of rat liver at 1.064 µm and 1.321 µm following photocoagulation. Lasers Surg. Med. 11, Suppl. 3: 5 (1991)
15. Yaroslavsky AN., Yaroslavsky IV., Goldbach T., Schwarzmaier HJ.: The optical properties of blood in the near infrared spectral range. Proc. SPIE 2678 (1996)
16. Reynolds L.: Diffuse reflectance from a finite blood medium: applications to the modeling of fiber optic catheters. Applied Optics, 15(9): 2059-2067 (1976)
17. Mie G.: Ann. d. Physik 25: 377 (1908)
18. Zijp JR., ten Bosch JJ.: Pascal program to perform Mie calculations. Optical Eng. 32(7):1691-1695 (1993)
19. MacRae RA., McClure A., Latimer P.: Spectral Transmission and Scattering Properties of Red Blood Cells. J.Opt.Soc.Am. 51(12):1366-1372 (1961)
20. Gordy E., Drabkin L.: Determination of the oxygen saturation of blood by a simplified technique applicable to standard equipment. J.Biol.Chem. 227: 285-299 (1957)
21. Steinke JM., Shepherd AP.: Effects of temperature on optical absorbance spectra of oxy-, carboxy-, and deoxyhemoglobin. Clin.Chem. 38(7):1360-1364 (1992)
22. Kuenstner JT., Norris KH.: Spectrophotometry of human hemoglobin in the near infrared region from 1000 to 2500 nm. J. Near Infrared Spectroscopy 2: 59-65 (1994)
23. Pittman RN.: In vivo photometric analysis of hemoglobin. Annals Biomed. Eng. 14: 119-137 (1986)
24. Steinke JM., Shepherd AP.: Diffusion model of the optical absorbance of whole blood. J.Opt.Soc.Am. A 5(6): 813-822 (1988)